NACA RM A52B13

NACA

RESEARCH MEMORANDUM

CASE FILE COPY

THE EFFECT OF BLUNTNESS ON THE DRAG OF SPHERICAL-TIPPED TRUNCATED CONES OF FINENESS RATIO 3 AT MACH NUMBERS 1.2 TO 7.4

By Simon C. Sommer and James A. Stark

Ames Aeronautical Laboratory
Moffett Field, Calif.

NATIONAL ADVISORY COMMITTEE FOR AERONAUTICS

WASHINGTON
April 25, 1952

NATIONAL ADVISORY COMMITTEE FOR AERONAUTICS

RESEARCH MEMORANDUM

THE EFFECT OF BLUNTNESS ON THE DRAG OF SPHERICAL-TIPPED TRUNCATED CONES OF FINENESS RATIO 3 AT MACH NUMBERS 1.2 TO 7.4

By Simon C. Sommer and James A. Stark

SUMMARY

The drag of spherically blunted conical models of fineness ratio 3 was investigated at Mach numbers from 1.2 to 7.4 in the Reynolds number range from 1.0×10^6 to 7.5×10^6. Results of the tests showed that slightly blunted models had less drag than cones of the same fineness ratio throughout the Mach number range. At Mach numbers less than 1.5, drag penalties due to large bluntnesses were moderate but these became severe with increasing Mach number.

Wave drag obtained by the method of Munk and Crown, in which the wave drag is determined by integrating the momentum loss through the head shock wave, showed that the wave drag and total drag followed the same trends with increasing bluntness. Wave drag was also estimated by combining the experimental wave drag of a hemisphere with the theoretical wave drag of a conical afterbody, and this estimate of wave drag is believed to be adequate for many engineering purposes.

INTRODUCTION

Blunt noses are being considered for some supersonic vehicles for the purpose of housing guidance equipment. In some cases a high degree of bluntness is required, and the drag penalty due to this bluntness may be significant. On the other hand, work done by others indicated that slightly blunt noses will have less drag than pointed noses of the same fineness ratio. For these two reasons the drag of blunt-nose shapes is of current interest and therefore an investigation was made in the Ames supersonic free-flight wind tunnel to determine the influence of bluntness on drag at Mach numbers from 1.2 to 7.4. The models tested were truncated cones with spherical noses having bluntness ratios of nose

diameter to base diameter from 0 to 0.50. All models had a fineness ratio of length to base diameter of 3.

SYMBOLS

A frontal area of model, square feet

C_D total drag coefficient $\left(\frac{\text{total drag}}{qA}\right)$

ΔC_D total drag penalty compared to the cone $\left(C_{D_{model}} - C_{D_{cone}}\right)$

C_{D_b} base drag coefficient $\left(\frac{\text{base drag}}{qA}\right)$

C_{D_f} skin-friction drag coefficient $\left(\frac{\text{skin-friction drag}}{qA}\right)$

C_{D_v} total drag coefficient based on volume to the two-thirds power $\left(\frac{\text{total drag}}{qV^{2/3}}\right)$

C_{D_w} wave drag coefficient $\left(\frac{\text{wave drag}}{qA}\right)$

d diameter of the base, feet

d_n diameter of the nose, feet

M free-stream Mach number

q free-stream dynamic pressure, pounds per square foot

R free-stream Reynolds number, based on axial length of model

V volume of model, cubic feet

MODELS

The models tested were truncated circular cones with tangentially connected spherical nose segments, as shown in figure 1(a). All models had a fineness ratio of 3, with base diameters and lengths of 0.45 and 1.35 inches, respectively. The models had holes bored in their bases for aerodynamic stability. Five different shapes were tested with nose diameters of 0, 7-1/2 percent, 15 percent, 30 percent, and 50 percent of the base diameter.

The models were constructed of 75-ST aluminum alloy. The maximum measured dimensional deviations were as follows: nose diameter, ±0.0005 inch; base diameter, ±0.0015 inch; length, ±0.020 inch; and the half-angle of the conical section, ±0.05°. For the majority of the models tested, the deviations were less than half of those given. The machined and polished surfaces had average peak to trough roughnesses of 20 microinches. In no case was there any correlation between the scatter of the test results and the dimensional deviations of the models.

TESTS AND EQUIPMENT

These tests were conducted in the Ames supersonic free-flight wind tunnel (reference 1) where models are fired from guns into still air or upstream into a supersonic air stream. The models were launched from a smooth-bore 20 mm gun, and were supported in the gun by plastic sabots (fig. 1(b)). Separation of the model from sabot was achieved by a muzzle constriction which retarded the sabot and allowed the model to proceed in free flight through the test section of the wind tunnel. Drag coefficient was obtained by recording the time-distance history of the flight of the model with the aid of a chronograph and four shadowgraph stations at 5-foot intervals along the test section. From these data, deceleration was computed and converted to drag coefficient.

With no air flow through the wind tunnel, Mach numbers varied from 1.2 to 4.2 depending on the model launching velocity. This condition is referred to as "air off." Reynolds number varied linearly with Mach number from 1.0×10^6 to 3.3×10^6, as shown in figure 2. With air flow established in the wind tunnel, referred to as "air on," the combined velocities of the model and Mach number 2 air stream, with the reduced speed of sound in the test section, provided test Mach numbers from 3.8 to 7.4. In this region of testing, Reynolds number was held approximately at 4×10^6 by controlling test-section static pressure. In addition, some models were tested at approximate Reynolds numbers of 3×10^6 and 7.5×10^6 at Mach number 6.

The purpose of this investigation was to obtain drag data near 0° angle of attack. This report includes only the data from models which had maximum observed angles of attack of less than 3° since larger angles measurably increased the drag.

Since there are no known systematic errors, the accuracy of the results is indicated by the repeatability of the data. Examination of these data shows that repeat firings of similar models under almost identical conditions of Reynolds number and Mach number yielded results for which the average deviation from the faired curve was 1 percent and the maximum deviation was 4 percent.

RESULTS AND DISCUSSION

Total Drag

Variation of the total drag coefficient with Mach number for each of the models tested is presented in figure 3. No attempt was made to join the air-off and air-on data due to differences in Reynolds number, recovery temperature, and stream turbulence. Variation of drag coefficient with Mach number for all models is similar, in that the drag coefficient continually decreased with increasing Mach number. There is, however, a tendency for the blunter models to show less decrease in drag coefficient with increasing Mach number.

These data have been cross-plotted in figure 4 to show the effect of bluntness on total drag coefficient for various Mach numbers. The nose bluntness for minimum drag shown by each curve decreases with increasing Mach number. This is shown by the dashed curve. At Mach number 1.2 the bluntness with minimum drag is 28 percent as compared to 11 percent at Mach number 7. At Mach numbers less than 1.5, drag penalties for models with bluntnesses approaching 50 percent are moderate but grow large with increasing Mach number. As Mach number becomes greater than 4.5, the drag penalties for large bluntnesses do not increase measurably but nevertheless are severe.

Drag in terms of volume may be important in some design considerations. In order to indicate the relative merit of the models in terms of drag for equal volume, the data of figure 4 have been replotted in figure 5, where drag coefficient is referred to volume to the two-thirds power. These curves show that moderate and even large bluntnesses (the degree of bluntness depending on Mach number) may be used to decrease the drag for equal volume.

Wave Drag

The variation of the total drag with model bluntness is believed to result primarily from the variation of the wave drag of the models and to be essentially independent of the base drag and skin-friction drag. In order to show this, the wave drag of the blunt models was estimated from the experiment by assuming the combined base drag and skin-friction drag independent of bluntness and these results were compared to wave drag determined by the method of Munk and Crown (reference 2). In the estimation of the wave drag, the base drag and skin-friction drag used were those of the cone, and were obtained by subtracting the theoretical wave drag of the cone (reference 3) from the experimental total drag of the cone at each Mach number. These values of combined base drag and

skin-friction drag were then subtracted from the total drag of the blunt models to obtain the wave drag of each model. The results are shown by the solid curves in figure 6, where wave drag is plotted as a function of model bluntness.

In the method of Munk and Crown, the wave drag is computed by summing up the momentum change through the head shock wave. Since part of the wave shape is unaccounted for because of the limited field of view in the shadowgraphs, an approximation suggested by Nucci (reference 4) was used to estimate the wave drag omitted. This approximation gives the upper and lower limits of the wave drag omitted. The mean value of these limits was used in all cases. These results are indicated by the points in figure 6. The mean disagreement between the results of this method and the results obtained by assuming base drag and skin-friction drag independent of bluntness is 7 percent.

Another method of estimating wave drag of the blunt models is by the addition of the wave drag of a hemisphere to that of a conical afterbody. Collected data showing the manner in which the wave drag of a hemisphere varies with Mach number is shown in figure 7.[1] The wave drag of the hemispherical tip was obtained directly from this figure, and the wave drag of the conical afterbody was obtained from the tables of reference 3. The results of this method are presented as the dashed curves in figure 6. A comparison of the results of this method with the results of the first two methods shows that although the method of estimating wave drag by the addition of the wave drag of a hemisphere to that of a conical afterbody appears to overestimate wave drag of the blunt models, it may nevertheless be adequate for many engineering purposes.

Viscous Effects

The effect of Reynolds number on total drag coefficient was investigated at Mach number 6. In figure 3, data for three Reynolds numbers,

---

[1]Wave drag of a hemisphere at Mach numbers from 1.05 to 1.40 was estimated from the data of reference 5 by calculating the wave drag of the pointed body and assuming that the drag due to the afterbody and fins was not a function of nose shape. At Mach numbers of 1.5, 2.0, 3.0, and 3.8, wave drag of a hemisphere was obtained from unpublished pressure distributions from the Ames 1- by 3-foot supersonic wind tunnel. Wave drag of a hemisphere at Mach numbers of 3.0, 4.5, 6.0, and 8.0 were estimated from total drag measurements of spheres (reference 6) by subtracting 70 percent of the maximum possible base drag and neglecting skin-friction drag. The possible error introduced by estimating the wave drag of the pointed body of reference 5 and the base drag of the sphere is believed to be no greater than ±4 percent.

3×10^6, 4×10^6, and 7.5×10^6 are included for cones and 50-percent blunt models. For the cones, the drag coefficient increased approximately 10 percent with increasing Reynolds number. For the 50-percent blunt models little or no change in drag coefficient was measured. The variation in drag coefficient for the cones was undoubtedly due to changes in the boundary-layer flow on the models at varying Reynolds numbers, as shown by the shadowgraphs in figure 8(a). At a Reynolds number of 3×10^6 the clearly defined wake (as indicated by the arrow in the figure) is associated with laminar flow. At high Reynolds numbers, the diffused wake indicates turbulent flow. Referring to figure 8(b), the boundary-layer wakes of the 50-percent blunt models appear diffused and turbulent at all Reynolds numbers. Since the wake of the 50-percent blunt model at Reynolds number of 3×10^6 appears turbulent compared to the laminar wake of the cone at this condition, it is concluded that boundary-layer transition occurred at lower Reynolds numbers on the 50-percent blunt model than on the cone.

An interesting flow phenomenon is illustrated in figure 9 by shadowgraphs of two cones at Mach number 3.7. The shadowgraph in figure 9(a) shows a smooth flow condition in contrast to a nonsteady disturbed flow condition shown in figure 9(b). The disturbed flow seems to consist of regions of turbulent air moving aft on the model surface, with pressure waves attached to the leading edges of these regions. Flow disturbance of this nature was observed occasionally on cones at small angles of attack at Reynolds numbers of 2.5×10^6 and greater. Cones with angles of attack in the order of 3° to 6° consistently had disturbed flow. This flow condition occurred less often on blunt models than on cones; and when present on blunt models, was always of slight intensity. Data for models that exhibited this flow condition were not included in this paper. The effect of flow disturbance on cones with angles of attack of less than 3° was to raise the drag about 8 percent. This increase in drag is attributed to increases in base drag as well as wave drag.

CONCLUSIONS

From this investigation, the following conclusions were drawn for spherically blunted conical models of fineness ratio 3:

1. Small amounts of spherical bluntness (nose diameters in the order of 15 percent of base diameter) have been found to be beneficial for reducing drag.

2. For large spherical bluntnesses (nose diameters in the order of 50 percent of base diameter) drag penalties were moderate at Mach numbers of less than 1.5, but became severe with increasing Mach number.

3. Estimation of wave drag by combining experimental values of wave drag of a hemisphere with wave drag of the conical surfaces is believed to predict wave drag adequately for many engineering purposes.

Ames Aeronautical Laboratory,
National Advisory Committee for Aeronautics,
Moffett Field, Calif.

REFERENCES

1. Seiff, Alvin, James, Carlton S., Canning, Thomas N., and Boissevain, Alfred G.: The Ames Supersonic Free-Flight Wind Tunnel. NACA RM A52A24, 1952.

2. Munk, Max M., and Crown, J. Conrad: The Head Shock Wave. Naval Ordnance Lab. Memo 9773, 1948.

3. Staff of the Computing Section, Center of Analysis, under the direction of Zdenek Kopal: Tables of Supersonic Flow Around Cones. M.I.T. Tech. Rep. No. 1, Cambridge, 1947.

4. Nucci, Louis M.: The External-Shock-Drag of Supersonic Inlets Having Subsonic Entrance Flow. NACA RM L50G14a, 1950.

5. Hart, Roger G.: Flight Investigation of the Drag of Round-Nosed Bodies of Revolution at Mach Numbers from 0.6 to 1.5 Using Rocket-Propelled Test Vehicles. NACA RM L51E25, 1951.

6. Hodges, A. J.: The Drag Coefficient of Very High Velocity Spheres. New Mexico School of Mines, Research and Devel. Div., Socorro, New Mexico, Oct. 1949.

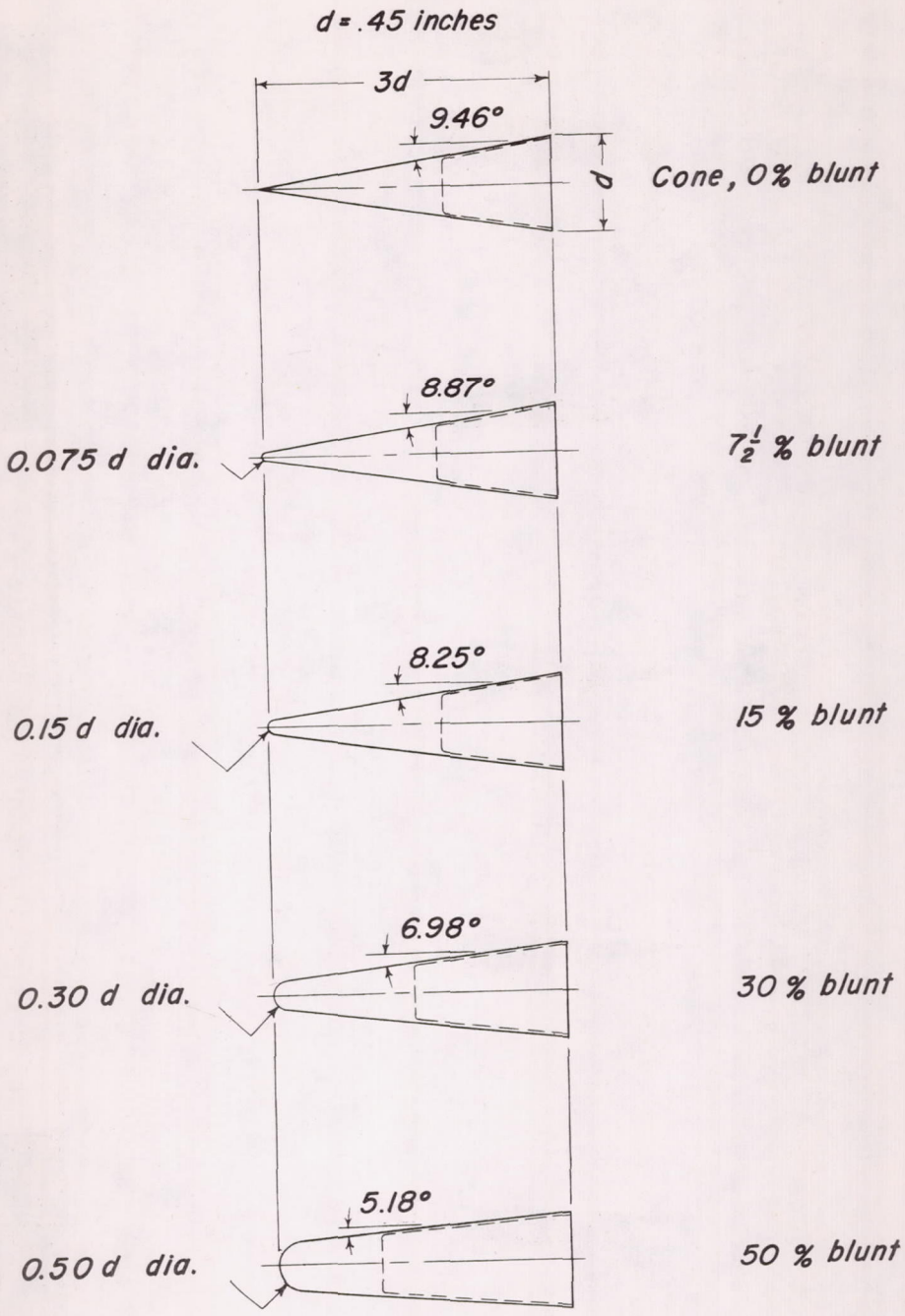

(a) Model geometry.

Figure 1.- Models tested.

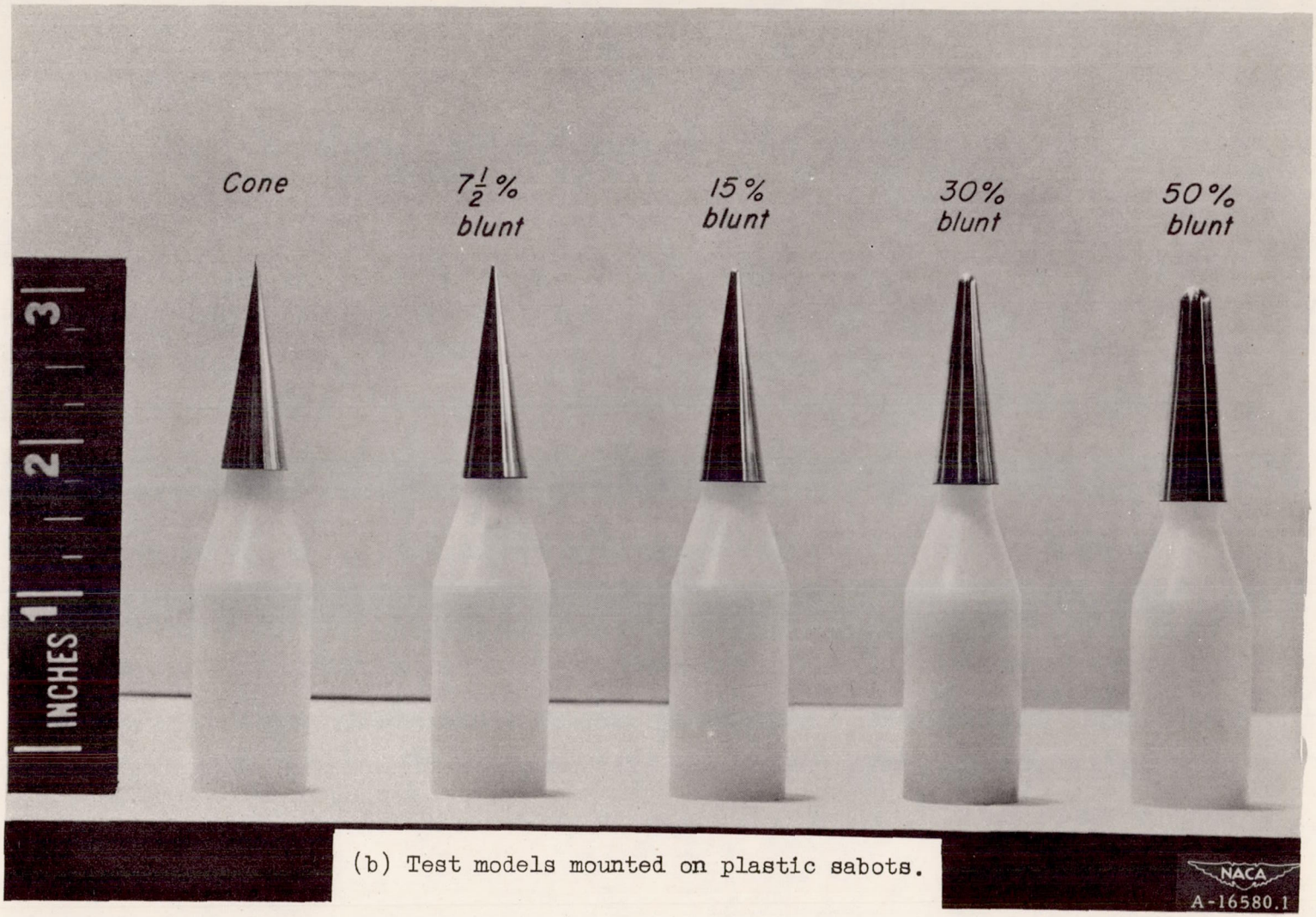

(b) Test models mounted on plastic sabots.

Figure 1.– Concluded.

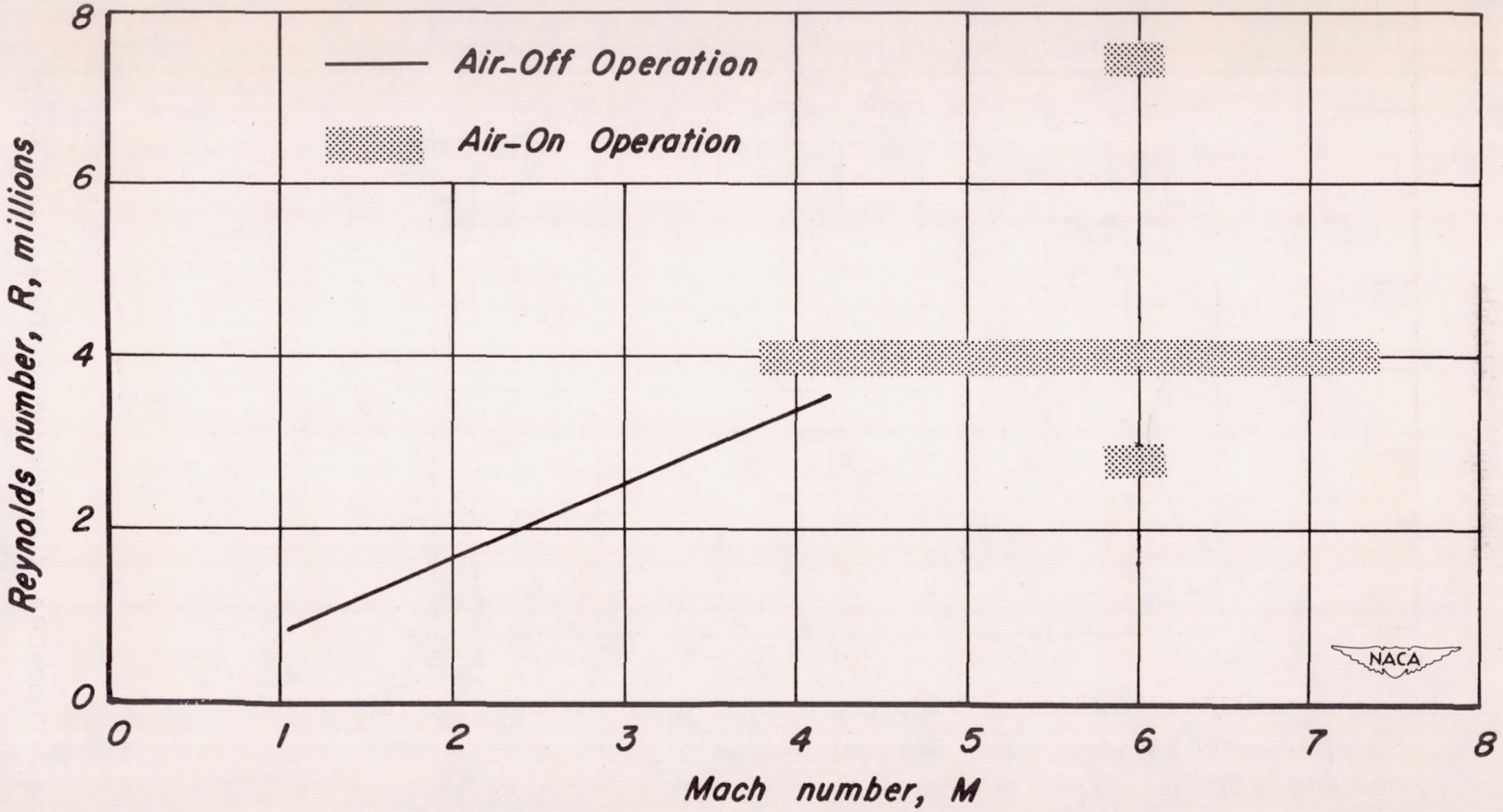

Figure 2.- Range of Mach numbers and Reynolds numbers of test.

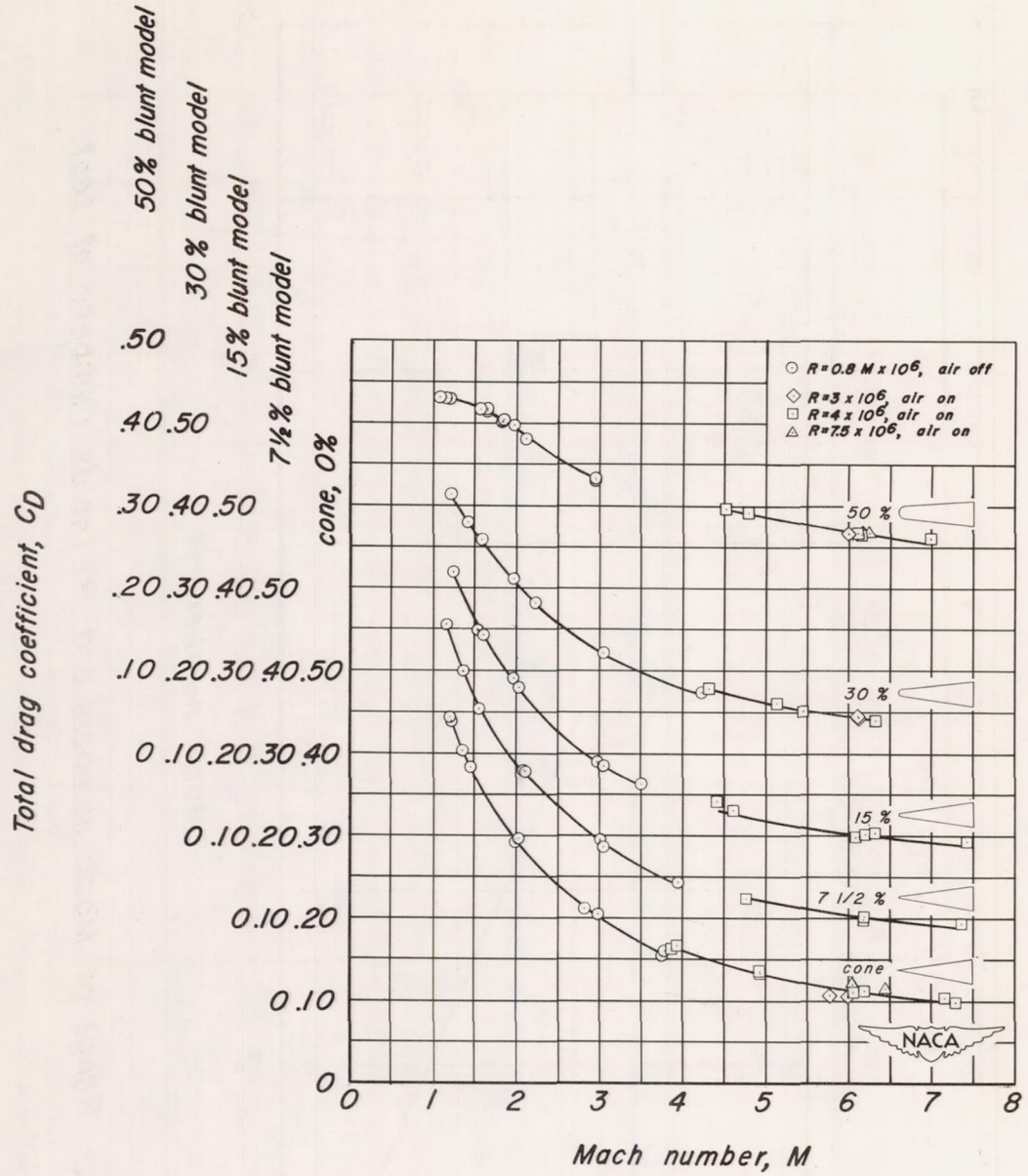

Figure 3.- Variation of total drag coefficient with Mach number.

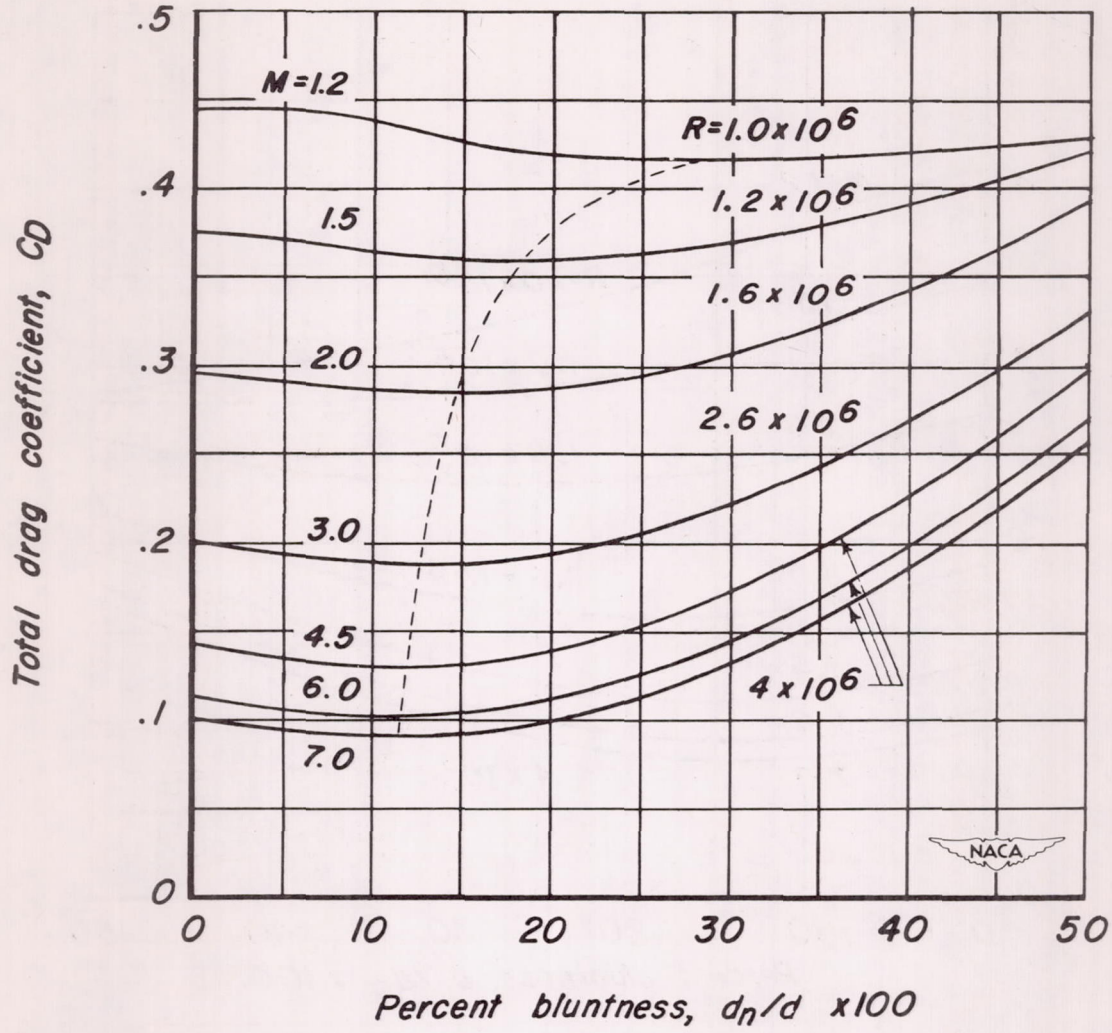

Figure 4.- The effect of bluntness on total drag coefficient.

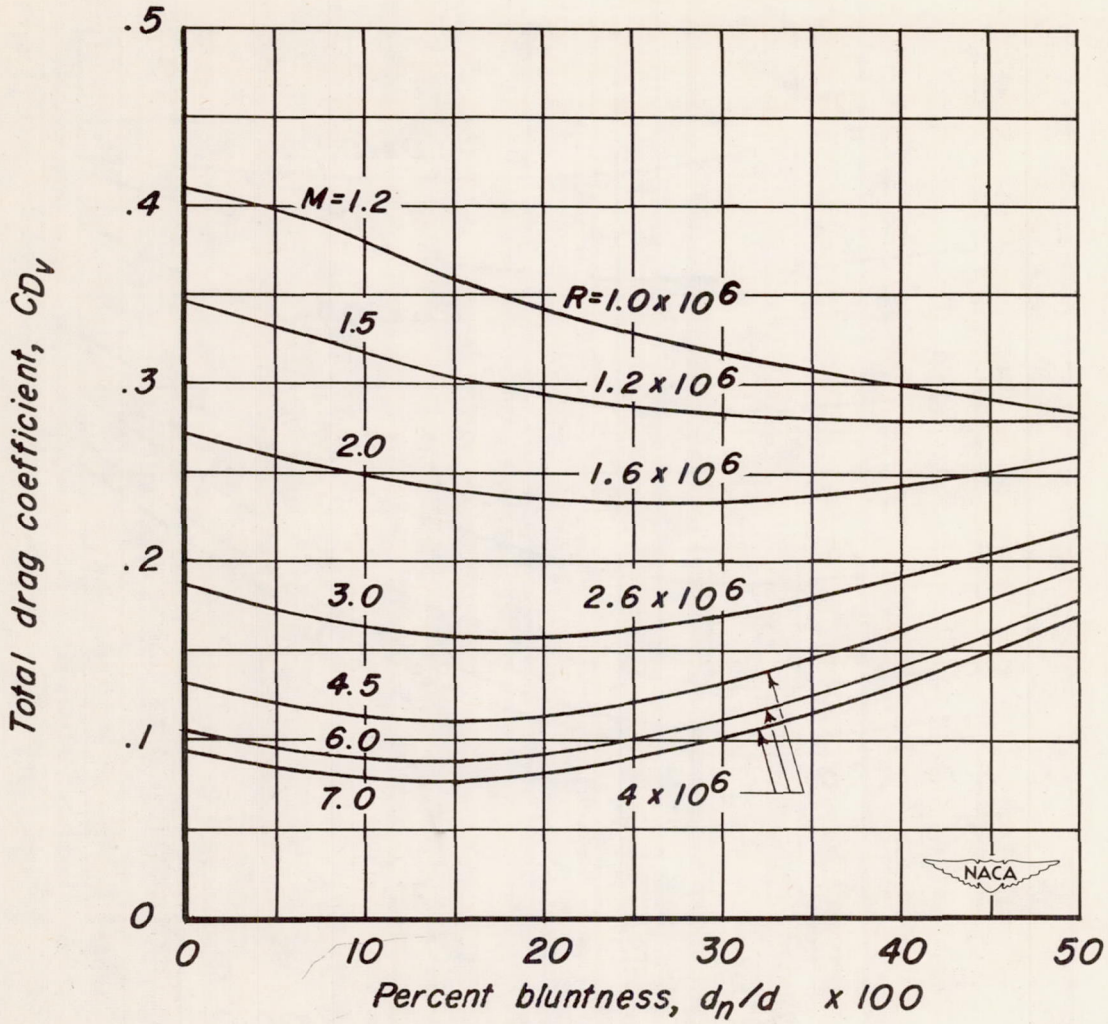

Figure 5.- The effect of bluntness on total drag coefficient based on volume to the two-thirds power.

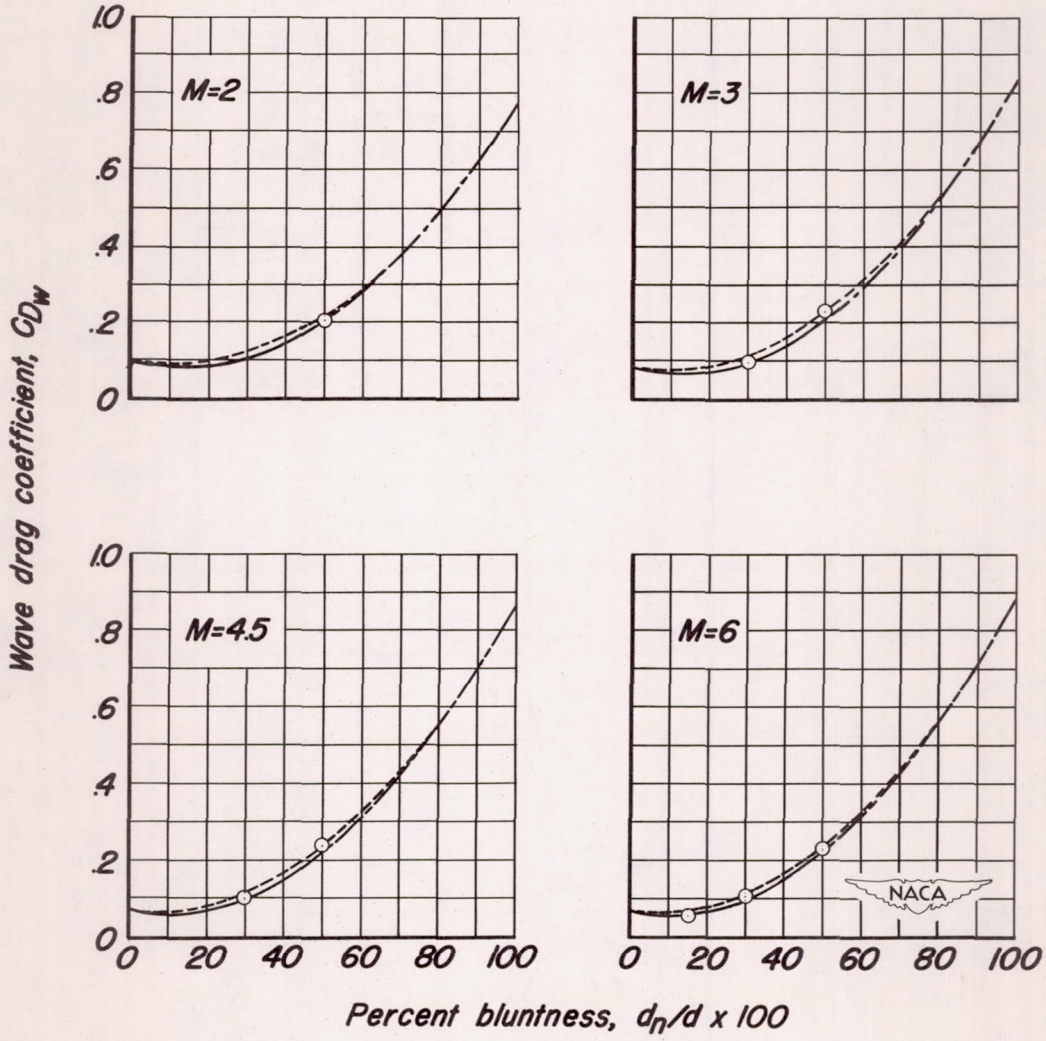

Figure 6.-Variation of wave drag coefficient with bluntness.

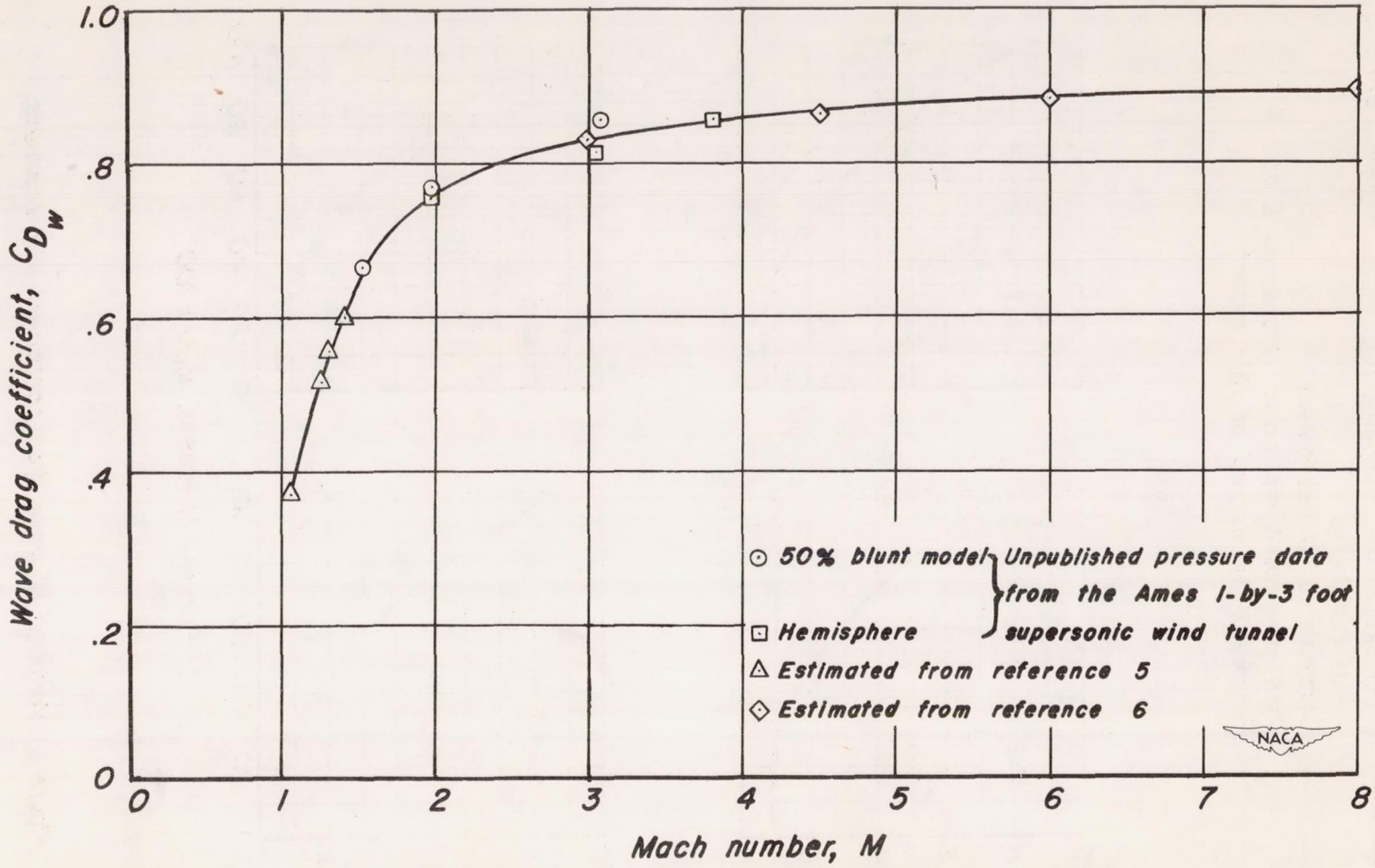

Figure 7.- Variation of wave drag coefficient with Mach number for a hemisphere.

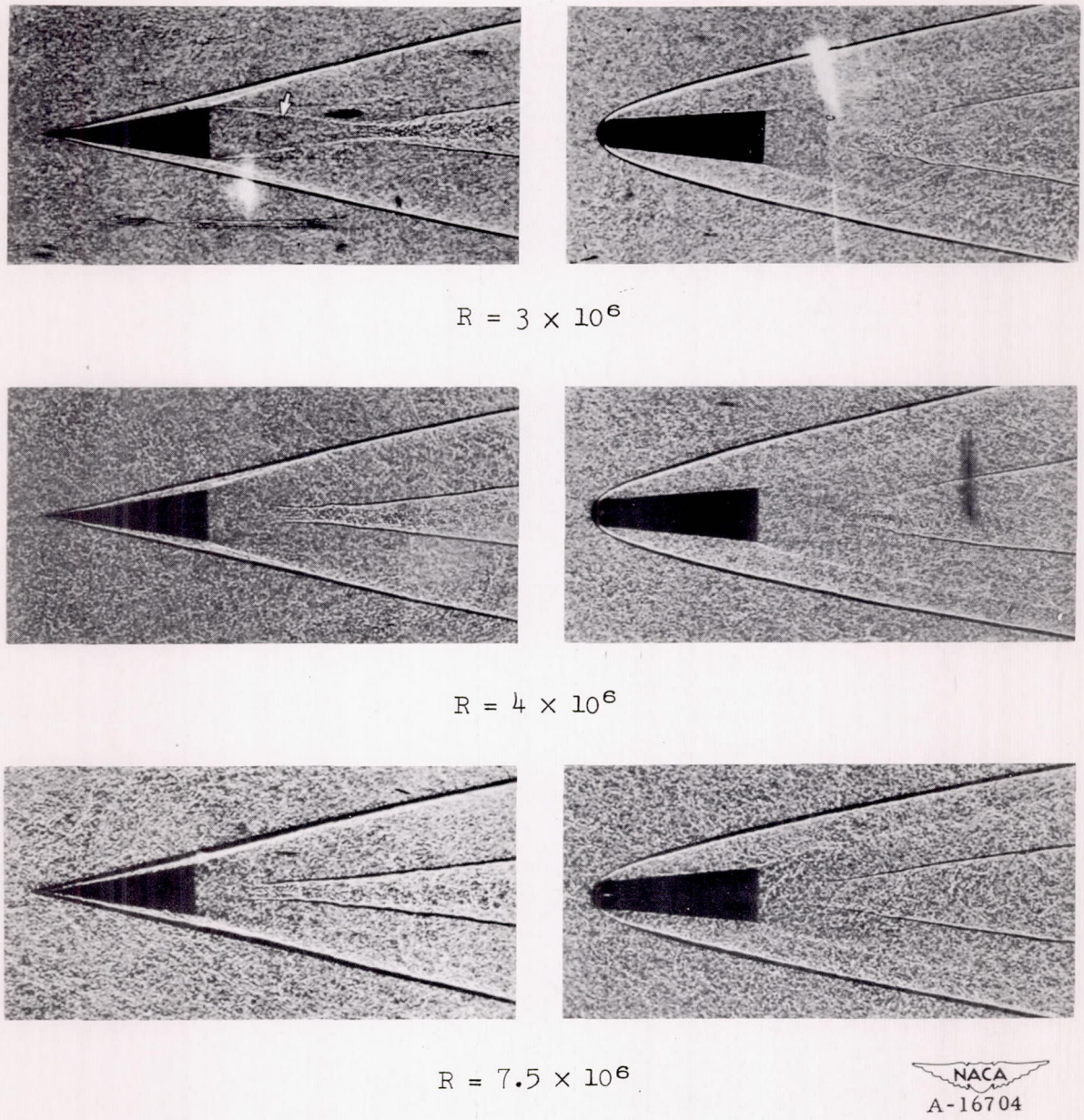

(a) Cones. (b) The 50-percent blunt models.

Figure 8.- Shadowgraphs of cones and 50-percent blunt models at Mach number 6.

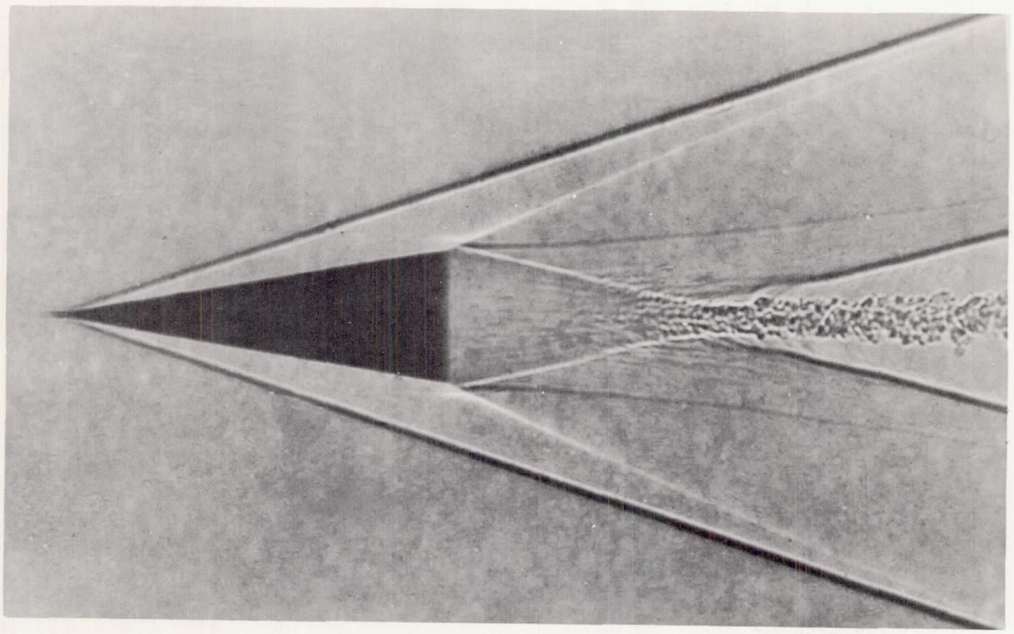

(a) Smooth flow.

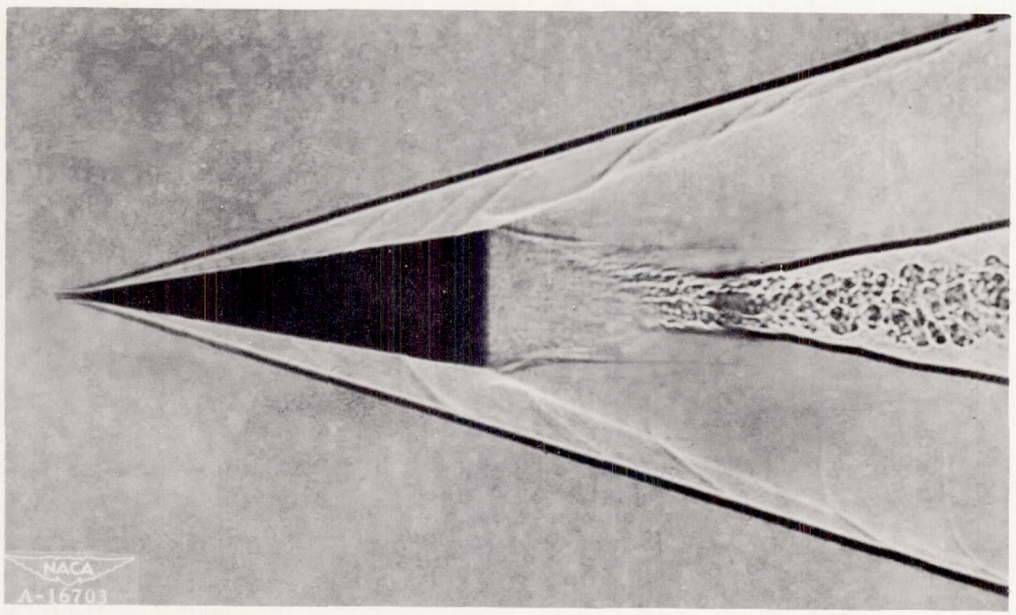

(b) Disturbed flow.

Figure 9.– Shadowgraphs comparing smooth flow with disturbed flow on cones at Mach number 3.7, Reynolds number of 3×10^6.